THE EFFECTS OF DIFFERENT ANNEALING TEMPERATURES AND NUMBER OF DEPOSITION LAYERS ON THE CRYSTALLOGRAPHIC PROPERTIES SODIUM NIOBATE (KNN) THIN FILMS SYNTHESIZED BY SOL-GEL SPIN COATING TECHNIQUE

M.H. Maziati Akmal[1,3], A.R.M. Warikh[1,4*], U.A.A. Azlan[2], N.A. Azmi[1]

[1]Faculty of Manufacturing Engineering, Universiti Teknikal Malaysia Melaka (UTeM), Hang Tuah Jaya, 76100 Durian Tunggal, Melaka, Malaysia.

[2]Faculty of Engineering Technology, Universiti Teknikal Malaysia Melaka (UTeM), Hang Tuah Jaya, 76100 Durian Tunggal, Melaka, Malaysia.
[3]Faculty of Engineering, International Islamic University Malaysia (IIUM), Jalan Gombak, 53100, Kuala Lumpur, Malaysia

[4]Tokushima-UTeM Academic Center, Tokushima University, 2-1 Minamo-Josanjima, 770-8506 Tokushima, Japan.

Email: [*1,4]warikh@utem.edu.my; [1,3]maziati.akmal1987@gmail.com; [2]umar@utem.edu.my; [1]azuwa.azmi@gmail.com

ABSTRACT: In this paper, the effects of different annealing temperature and number of deposition layers on the crystallographic properties of potassium sodium niobate (KNN) thin films were investigated. X-ray diffraction (XRD) analysis was carried out to determine the crystallographic orientation and phase formation of thin films deposited at different annealing temperatures (600°C, 650°C and 700°C) and various number of deposition layers (1, 2, 3, 4 and 4 layers). The XRD patterns and texture coefficient of the synthesized films confirmed that a highly oriented orthorhombic perovskite structure was obtained at 650°C, while at higher temperature a spurious phase of $K_4Nb_6O_{17}$ was evolved. The effective number of deposition layers was found to be five due to the formation of interconnected cracks at sixth deposited layers. The XPPA analysis showed that the unit cell volume of the films was increased gradually from 110.83 cm^3 at one layer to 124.31 cm^3 at fifth deposited layers. Nevertheless, the lattice strain effect was small and negligible at high layer deposition due to the increased distance of the lattice with the film/substrate interface.

KEYWORDS: *KNN; film; sol-gel spin coating; crystallographic; deposition layer*.

1.0   INTRODUCTION

The development of safe piezoelectric materials is particularly important in fulfilling the market's demand because the toxicity of lead-based materials makes them detrimental to be used in microelectromechanical systems (MEMS) [1], [2]. Hence, lead-free piezoelectric ceramic, namely potassium sodium niobate, $K_{0.5}Na_{0.5}NbO_3$ (KNN) which exhibits strong piezoelectric response and good mechanical properties became a widely investigated material for MEMS applications like actuators, transducers, modulators and sensors [1], [3], [4]. One advantage of KNN over conventional lead-based materials is that a high Curie temperature (420 ^{o}C) allows the material's stability to be enhanced, thus improving its piezoelectric properties [5], [6]. While KNN bulk ceramics have already been studied for potential applications, a real game-changing technology would be the development of KNN thin films for flexible integration and miniaturization in MEMS [7], [8]. Hence, various thin films deposition techniques have been explored such as radio frequency magnetron sputtering [9], pulse laser deposition [10] and sol-gel spin coating [11]. Among these, the sol-gel spin coating is regarded as the most facile process due to its simplicity [12]. Moreover, spin-coating method can produce uniform films comparable with other PVD techniques. In practice, more than a single layer of coating is needed to produce high-quality thin films that are highly crystalline and cracks-free [13]. Additionally, the film's quality is also affected by thermal treatments such as pyrolysis and and annealing temperature [14], [15].

Due to the various synthetic routes adopted for films synthesis, particle size and crystal morphology would also be affected. Theoretically, no crystals are perfect considering their infinite size [16]. Crystal imperfection might cause the deviation of peak diffractions broadening the materials. The diffraction peaks of materials can be used to analyze the lattice strain within the crystal structure. The lattice strain is a manifestation of a change in the lattice constants arising from crystal imperfection, such as lattice dislocation or lattice mismatch. The effect of lattice strain can be observed in the thin film as compared to bulk materials due to film/substrate mismatch.   Numerous indirect techniques can be employed for determining lattice strains which are direct light scattering (DLS),

transmission electron microscopy and X-ray peak profile analysis (XPPA). Though XPPA is based on mathematical and averaging methods, it's still considered a simple and powerful technique for crystal size and strain determination [17].

It should be mentioned that most of the studies on KNN thin films prepared by sol gel spin coating method were focused on their piezoelectric properties, and no reports have been dedicated on the studies of their processing parameters. Hence, in this study, the effects of different annealing temperature and the number of layers on the crystallographic properties of KNN were analysed to determine the optimum processing conditions for best experimental practice. XRD was used to analyze the formation of phase and crystallographic properties of KNN thin films. The lattice strain and lattice parameter were then investigated by XPPA.

2.0   METHODOLOGY

Two experimental designs were outlined in this part. The first part describes a facile route to produce KNN films while the next part includes the characterization method of KNN films to obtain its lattice parameter.

2.1   Preparation of KNN films

The KNN solutions were prepared using sol-gel synthesis. Two alkaline precursors, namely potassium acetate (Alfa Aesar, 99 % purity) and sodium acetate (Alfa Aesar, 99 % purity), were used as starting solutions. The stoichiometry of reactants taken is K: Na: Nb (0.5: 0.5: 1) which is in mol%. These chemicals were dissolved in 20 ml of 2-methyoxyethanol (Sigma-Aldrich, 99.9 % purity) and constantly stirred at room temperature of ~25 °C for 30 minutes. Separately, 0.627 mL of niobium (V) ethoxide (Sigma Aldrich, 99.5 % purity) was dissolved by constantly stirring in a mixed solution of 10 mL 2-methyoxyethanol and 0.156 mL acetylacetone Sigma- Aldrich, > 99.9 % purity) for 30 minutes. After stirring vigorously for 30 minutes at room temperature, a mixed solution of niobium ethoxide and acetylacetone was added dropwise to the prepared KN precursors.

The ensuing mixture was left to stand for an hour at 80 °C to create a clear and homogenous solution. The thin films were then produced when the mixed solution was spun onto the Si substrate at 3000 rpm for 30 seconds. This was followed with pyrolysis where the wet films were dried at 250 °C for 1 minute to remove organic contaminant. The spin coating and pyrolysis processes were done repeatedly till well-defined films of a certain thickness were obtained. Following this, the films were annealed at various temperatures using rapid thermal annealing furnace (RTP-1000D4, MTI) at a rate of 5°C/s for 5 minutes.

2.2   Characterization methods

XRD was used to analyze the formation of phase and crystallographic properties of KNN thin films using PANanalytical X'Pert Pro3. The scanning speed was set up to 0.05 °C/s using u Kα radiation. The 2θ scan range was from 20° to 70°. For the thin films, the grazing angle was used to render the XRD measurement more sensitive to the interesting surface region and eliminate substrate contribution on the diffraction response. Therefore, the angle was set to 0.1°. The surface morphology of the thin film was examined using field emission scanning electron microscopy (FESEM, Hitachi 51400) operating at 10 kV.

3.0   RESULTS AND DISCUSSION

Figure 1 shows the recorded XRD diffraction patterns of KNN films annealed at 600 °C, 650 °C and 700 °C. The peaks of KNN thin films annealed at 600 °C and 650 °C were indexed by the orthorhombic perovskite sructure of KNN (JCPDS No. 32-0822) as shown in Figure 1. The presence of multiple peaks indicates that the grown films are polycrystalline in nature, which agrees well with other findings [18], [19], [20]. As can be seen, the KNN film grown at 600 °C had a pure orthorhombic perovskite structure with no secondary phase detected. As the temperature was raised to 650 °C, the intensity and the integrity of the peaks were increased. However, the peaks of the film annealed at 700 °C are shifted to the new angle which indicates the formation of pyrochlore phase of $K_4Nb_6O_{17}$ tungsten bronze structure. This observation is supported by Fernandes who discovered the existence of non-perovskite phase of $K_4Nb_6O_{17}$ due to rapid

volatilization of the alkaline element at an elevated temperature [21]. Furthermore, Ahn et al. [22] reported that the higher volatilization rate of Na^+ than K^+ during heat treatment would cause the formation of this secondary phase which subsequently deteriorate the structural and piezoelectric properties of KNN.
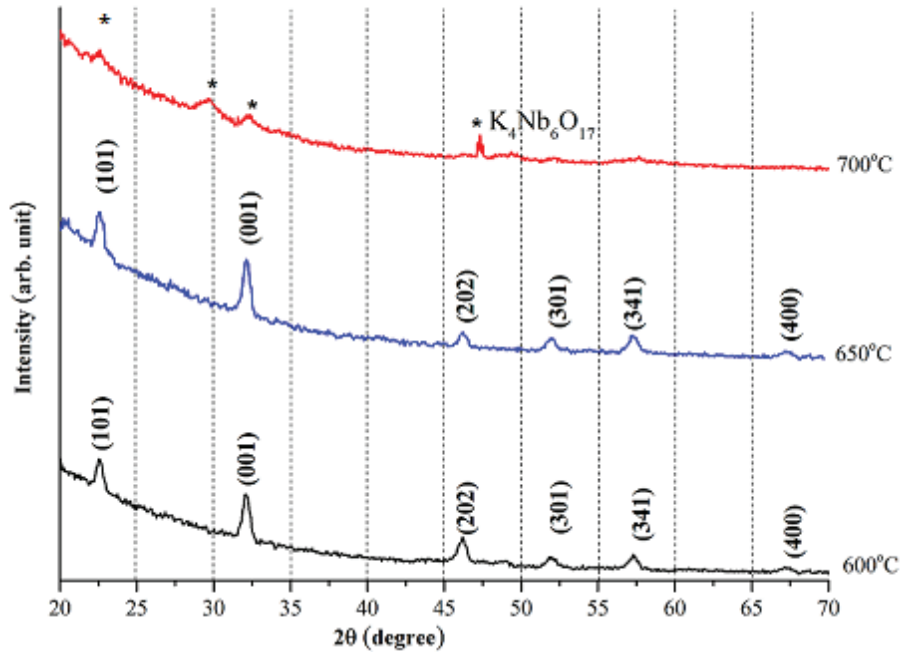

Figure 1: XRD spectra of KNN thin films annealed at different temperature

As mentioned previously, the film annealed at 700 °C displays the formation of undesirable pyrochlore phase. Thus, only the annealed samples with orthorhombic structure were considered for the texture coefficients (TC) evaluation. TC values can be calculated using Equation 1 [16] to obtain quantitative information regarding the preferential crystal orientation.

$$\text{TC}_{hkl} = \frac{I_{(hkl)}}{I_{0(hkl)}} / N^{-1} \sum_n \frac{I_{(hkl)}}{I_{0(hkl)}} \qquad (1)$$

where $TC_{(hkl)}$ is the texture coefficient, I_{hkl} is the intensity of the sample , N is the number of peaks diffracted and I_o is the intensity of XRD reference. If TC $_{(hkl)}$ for all indexed planes (hkl) is close to unity, then the crystallites indicate similar orientation to the JCPDS reference, while values greater than 1 indicate the abundance of grains oriented in the <hkl> direction. Table 1 provides the TC $_{(hkl)}$ value of KNN samples. It can be seen that, TC $_{(hkl)}$ for grown films improved as temperature increased to 650 °C, thus indicating the preferential growth of crystallites at this temperature. The improved peak intensity and greater $TC_{(hkl)}$ value clearly suggest that the KNN film annealed at 650 °C achieved the optimum crystallization in

annealed at 650 °C achieved the optimum crystallization in comparison with other films. Hence, this temperature was used for deposition of subsequent films.

Table 1: Texture coefficients value of KNN films annealed at differe temperature

Annealing temperature	TC_{101}	TC_{001}	TC_{202}	TC_{301}	TC_{341}	TC
600 °C	1.321	2.031	0.856	0.127	0.411	0.0
650 °C	1.703	2.834	1.252	0.239	0.576	0.1

Figure 2 shows the XRD patterns of KNN films with dif coating layers. As anticipated, the XRD spectra of the thin filr similar to an orthorhombic perovskite structure with no evide secondary phase. Under the same annealing temperature intensity of the peaks is increased with increasing coating

with the preferred orientation at (001). The result implie crystalline quality is improved with an increasing number of la
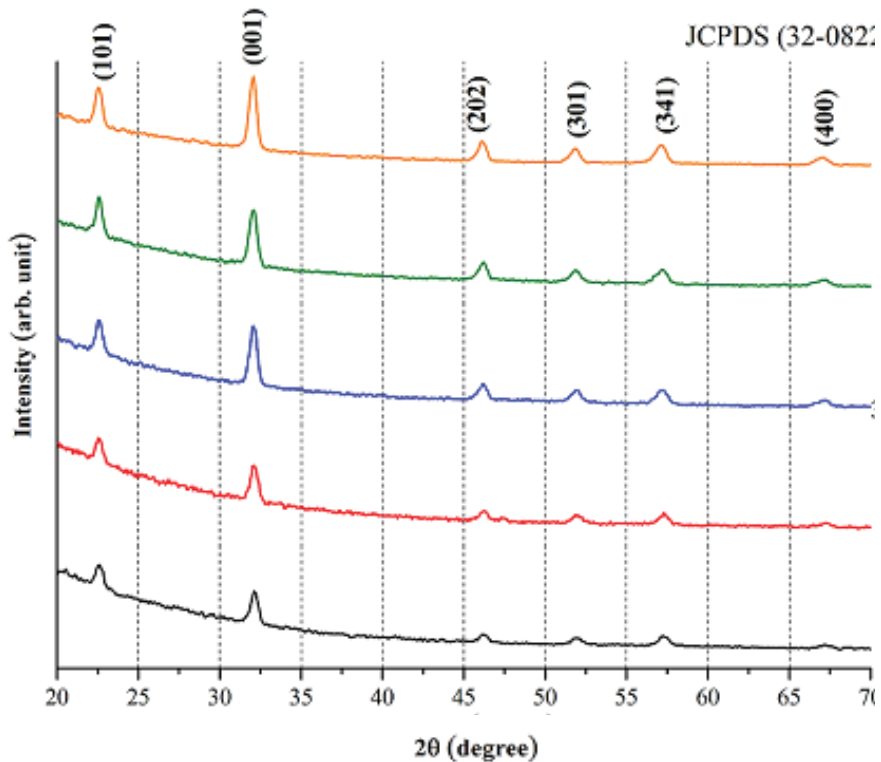

Figure 2: XRD spectra of KNN thin films

due to different of crystal planes and lattice symmetries between the substrate and the film [23]. The lattice mismatch between substrate and film causes in-plane tensile or compressive strain in the deposited layer. Due to thin films deposited on a crystalline substrate, there also will be a biaxial strain to accommodate the lattice mismatch (Figure 3b). Thus, it is suggested that the strain will occur in the multilayer film.

Table 2: The lattice parameters of the synthesized samples

Thin film layers	Space group	Lattice parameters		
		a (Å)	c (Å)	Volume (Å)
1 layer	(Cm2m)	3.811	5.470	110.83
2 layers	(Cm2m)	3.834	5.495	114.14
3 layers	(Cm2m)	3.853	5.507	117.06
4 layers	(Cm2m)	3.843	5.641	119.66
5 layers	(Cm2m)	3.913	5.649	124.31

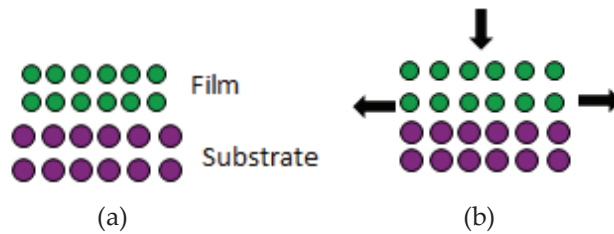(a)   (b)

Figure 3:   a) Lattice misfit   (b) Strain in film for mismatch accommodation

To estimate the strain that occurs within the lattice structure, an X-ray peak profile analysis (XPPA) was employed. This method considers a number of diffraction peaks from the XRD pattern and was further evaluated by Gaussian and Lorentzian function which is given by [24]:

$$(d_{hkl}\beta_{hkl}\cos\theta)^2 = \frac{K}{D}(d_{hkl}^2\beta_{hkl}\cos\theta) + \left(\frac{\varepsilon}{2}\right)^2 \qquad (2)$$

where d_{hkl} is the lattice spacing, β_{hkl} is the integral half width, K is the lattice constant (0.90) and D is the crystallite size, respectively. To evaluate the lattice strain, the mathematical expression $(d\beta\cos\theta)^2$ was plotted against $d^2\beta\cos\theta$ as illustrated in Figure 4. The obtained points were then linearly fitted using linear regression, R^2, to minimize the error of estimation. It is worth noting that the reliability of the data is increased in the case of R^2 >0.8, which would reduce the weak persuasion and error of the data. The lattice strain was further

obtained from the y-intercept of linearly fitted data. The result is schematically presented in Figure 5. Interestingly, it can be seen that strain decreases along with the number of deposition layers from 7.5 at 1st layer to 5.3 at 5th layers, respectively. According to Tealdi et al. , the significant reduction in strain is due to the greater distance of the strain released from the film/substrate interface [24]. As a result, the effects of lattice strain at a high deposition layer became small and negligible.
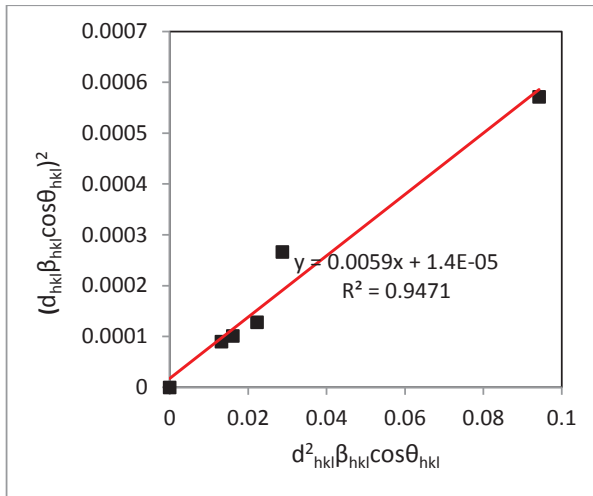

Figure 4: Graphic representation of XPPA method for lattice strain calculation
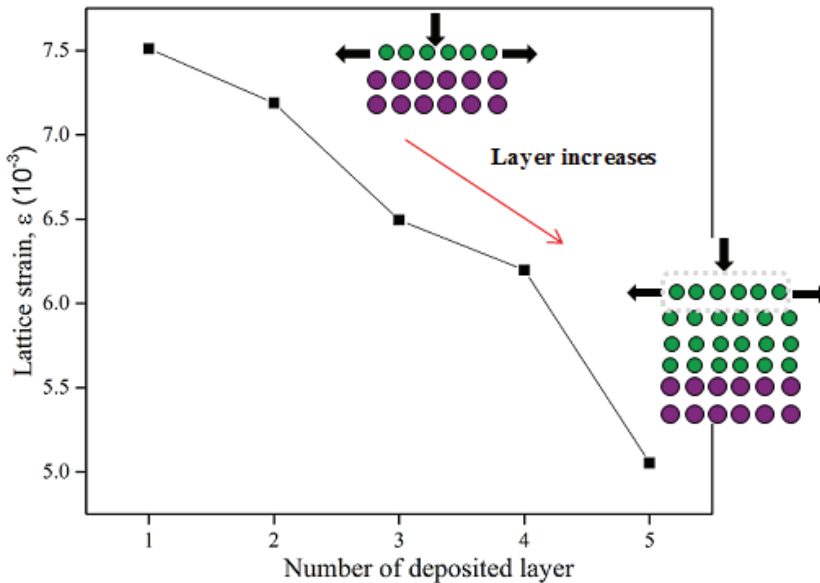

Figure 5: The apparent change in the lattice strain as a function of deposition

improve the film properties. It was discovered that the number of layers that could be sustained was only up to five layers. When the number of layers was extended to six, the cracks evolved on the structure of the film as shown in Figure 2. These cracks, also known as "mud cracks," resemble the pattern of a dry lake bed. It should be noted that above the critical coating thickness, repetitive heating or pyrolysis treatment causes the thermal expansion of the films exceeded the substrates, resulting in the propagation and evolution of cracks as shown in Figure 2 [13], [25].
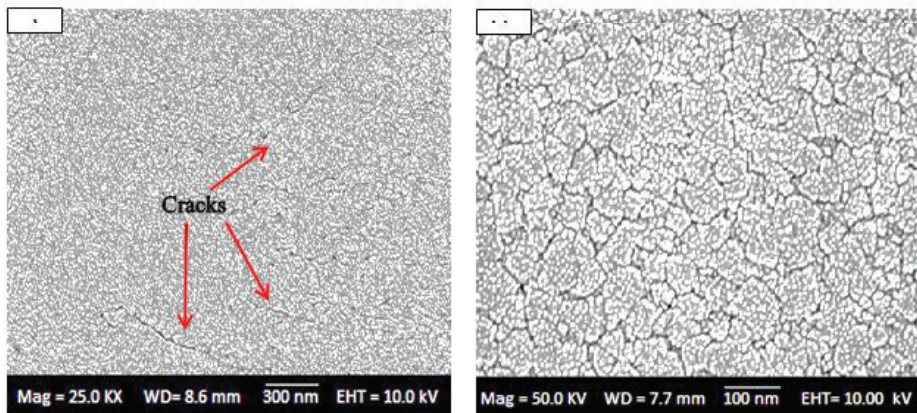

Figure 6: Evolution of interconnected cracks with six deposition layer
a) 25.0 Kx b) 50.0Kx

4.0   C O N C L U S I O N

KNN thin films were prepared on Si substrate by sol-gel spin coating method. The optimum annealing temperature and deposition layers were found to be 650°C and five deposition layers, respectively . It was found that the KNN films were mainly composed of a pure orthorhombic perovskite structure. The crystalline quality was observed to be improved by increasing the number of layers up to five. Nonetheless, it was discovered that KNN film with six deposition layer exhibited the interconnected cracks. Based on the XPPA, the strain of the lattice decreased significantly, while the unit cell volume steadily increased when the number of layers increased. These results clearly show that the annealing temperature and deposition layers predominantly affect the phase formation and crystallographic properties of KNN thin films.

ACKNOWLEDGEMENTS

REFERENCES

[1]   L. Zhengfa, L. Yongxiang, and Z. Jiwei, "Grain growth and piezoelectric property of KNN-based lead-free ceramics," *Curr. Appl. Phys.*, vol. 11, no. 3, pp. S2–S13, 2011.

[2]   P. Kumari, R. Rai, S. Sharma, M. Shandilya, and A. Tiwari, "State-of-the-art of lead free ferroelectrics: A critical review," vol. 6, no. 6, pp. 453–484, 2015.

[3]   M.A.M. Hartar, M.W.A. Rashid and A.U.A. Amani, "Physical an electrical properties enhancement of rare-earth doped-potassium sodium niobate (KNN): A review: *J. Ceramics-Silikaty.*, vol. 59, no. 2, pp. 158-163. 2015.

[4]   C.H. Hong, H.-P. Kim, B.-Y. Choi, H.-S. Han, J. S. Son, C. W. Ahn, and W. Jo, "Lead-free piezoceramics – Where to move on?," *J. Mater.*, vol. 2, no. 1, pp. 1–24, 2016.

[5]   J. Du, J. Wang, G. Zang, and X. Yi, "Phase transition behavior and piezoelectric properties of low-Li and high-Sb modified KNN based piezoceramics," *Phys. B Condens. Matter*, vol. 406, no. 21, pp. 4077–4079, Nov. 2011.

[6]   M. H. M. Akmal, A. R. M. Warikh, U. A. A. Azlan, M. A. Azam, and S. Ismail, "Effect of amphoteric dopant on the dielectric and structural properties of yttrium doped potassium sodium niobate thin film," *Mater. Lett.*, vol. 170, pp. 10–14, May 2016.

[7]   D. Fasquelle, M. Mascot, N. Sama, D. Remiens, and J.-C. Carru, "Lead-free piezoelectric thin films for RoHS devices," *Sensors Actuators A Phys.*, vol. 229, pp. 30–35, Jun. 2015.

[8]   R. Anthony, C. O' Mathúna, and J. F. Rohan, "MEMS based electrochemical process for fabrication of laminated micro-inductors on silicon," *Microelectron. Eng.*, vol. 155, pp. 33–38,

Apr. 2016.

[9]   T. Li, G. Wang, K. Li, G. Du, Y. Chen, Z. Zhou, and D. SRO / STO by RF magnetron sputtering," *Ceram. Int.*, vol. 40, no. 1, pp. 1195–1198, 2014.

[10]   M. Zhu, X. Shang, G. Chang, M. Li, X. Liu, T. Zhou, and Y. He, "Pulsed laser deposition of single-phase lead-free NKLNST thin films with K- and Na-excess targets," *J. Alloys Compd.*, vol. 567, pp. 97–101, Aug. 2013.

[11]   L. Wang, W. Ren, K. Yao, P. C. Goh, P. Shi, X. Wu, and X. Yao, "Effect of Pyrolysis Temperature on $K_{0.5}Na_{0.5}NbO_3$ Thick Films Derived from Polyvinylpyrrolidone-Modified Chemical Solution," *J. Am. Ceram. Soc.*, vol. 93, no. 11, pp. 3686–3690, Nov. 2010.

[12]   G. H. Khorrami, a. Kompany, and a. Khorsand Zak, "Structural and optical properties of $(K,Na)NbO_3$ nanoparticles synthesized by a modified sol–gel method using starch media," *Adv. Powder Technol.*, vol. 26, no. 1, pp. 113–118, Jan. 2015.

[13]   J. H. Prosser, T. Brugarolas, S. Lee, A. J. Nolte, and D. Lee, "Avoiding cracks in nanoparticle films," *Nano Lett.*, vol. 12, no. 10, pp. 5287–5291, 2012.

[14]   Q. Yu, J.-F. Li, Y. Chen, L.-Q. Cheng, W. Sun, Z. Zhou, and Z. Wang, "Effect of Pyrolysis Temperature on Sol-Gel Synthesis of Lead-free Piezoelectric $(K,Na)NbO_3$ Films on $Nb:SrTiO_3$ Substrates," *J. Am. Ceram. Soc.*, vol. 97, no. 1, pp. 107–113, Jan. 2014.

[15]   A. A. Akl, "Thermal annealing effect on the crystallization and optical dispersion of sprayed V_2O_5 thin films," *J. Phys. Chem. Solids*, vol. 71, no. 3, pp. 223–229, Mar. 2010.

[16]   P. Bindu and S. Thomas, "Estimation of lattice strain in ZnO nanoparticles: X-ray peak profile analysis," *J. Theor. Appl. Phys.*, vol. 8, no. 4, pp. 123–134, Jul. 2014.

[17]   B. D. Cullity, "Elements of X-Ray Diffraction," *Am. J. Phys.*, vol. 25, no. 6, p. 394, 1957.

[18]   G. H. Khorrami, A. Kompany, and A. Khorsand Zak, "A facile sol-gel approach to synthesize KNN nanoparticles at low temperature," *Mater. Lett.*, vol. 110, pp. 172–175, 2013.

[19]   N. Li, W. L. Li, L. D. Wang, D. Xu, Q. G. Chi, and W. D. Fei, "Improved leakage property and reduced crystallization temperature by V2O5 seed layer in K0.4Na0.6NbO3 thin films derived from chemical solution deposition," *J. Alloys Compd.*, vol. 552, pp. 269–273, Mar. 2013.

[20]   M. H. M. Akmal, A. R. M. Warikh, U. A. A. Azlan, M. A. Azam, T.J.S. Anand and T.Moriga, "Structural evolution and dopant occupancy preference of yittrium-doped potassium sodium niobate thin films," *J. Electroceramics*, pp. 1-8, 2016.

[21]   A. F. Solarte, N. Pellegri, O. De Sanctis, and M. G. Stachiotti, "Simple and Rapid Fabrication of Na $_{0.5}$ K $_{0.5}$ NbO $_3$ Thin Films by a Chelate Route," vol. 2013, 2013.

[22]   C.W. Ahn, H.-I. Hwang, K. S. Lee, B. M. Jin, S. Park, G. Park, D. Yoon, H. Cheong, H. J. Lee, and I. W. Kim, "Raman Spectra Study of K $_{0.5}$ Na $_{0.5}$ NbO $_3$ Ferroelectric Thin Films," *Jpn. J. Appl. Phys* C.., vol. 49, no. 9, p. 95801, 2010.

[23]   C. Tealdi, J. Heath, and M. S. Islam, "Feeling the strain: enhancing ionic transport in olivine phosphate cathodes for Li- and Na-ion batteries through strain effects," *J. Mater. Chem. A*, vol. 4, no. 18, pp. 6998–7004, 2016.

[24]   G. H. Khorrami, a. Khorsand Zak, a. Kompany, and R. Yousefi, "Optical and structural properties of X-doped (X=Mn, Mg, and Zn) PZT nanoparticles by Kramers–Kronig and size strain plot methods," *Ceram. Int.*, vol. 38, no. 7, pp. 5683–5690, Sep. 2012.

[25]   Z. C. Xia and J. W. Hutchinson, "Crack patterns in thin films," *J. Mech. Phys. Solids*, vol. 48, no. 6, pp. 1107–1131, 2000.